REGULAR ARTICLE

blood advances

Identification of a murine CD45^{-}F4/80^{lo} HSC-derived marrow endosteal cell associated with donor stem cell engraftment

Kathleen M. Overholt,[1,2] Satoru Otsuru,[1] Timothy S. Olson,[3] Adam J. Guess,[1] Victoria M. Velazquez,[1] Laura Desbourdes,[1] Massimo Dominici,[4] and Edwin M. Horwitz[1,2,5]

[1]Center for Childhood Cancer and Blood Diseases, The Research Institute, and [2]Department of Pediatric Hematology, Oncology, and Bone Marrow Transplantation, Nationwide Children's Hospital, Columbus, OH; [3]Children's Hospital of Philadelphia, Philadelphia, PA; [4]University Hospital of Modena and Reggio, Emilia, Modena, Italy; and [5]Department of Medicine, The Ohio State University, Columbus, OH

Key Points

- Novel CD45^{-}F4/80^{lo} marrow cells are developmentally derived from hematopoietic progenitors and reside among the endosteal osteoblasts.
- In situ depletion of CD45 cells before marrow radioablation results in flattened osteoblasts and absent HSC engraftment.

Hematopoietic stem cells (HSCs) reside in specialized microenvironments within the marrow designated as stem cell niches, which function to support HSCs at homeostasis and promote HSC engraftment after radioablation. We previously identified marrow space remodeling after hematopoietic ablation, including osteoblast thickening, osteoblast proliferation, and megakaryocyte migration to the endosteum, which is critical for effective engraftment of donor HSCs. To further evaluate the impact of hematopoietic cells on marrow remodeling, we used a transgenic mouse model (CD45Cre/iDTR) to selectively deplete hematopoietic cells in situ. Depletion of hematopoietic cells immediately before radioablation and hematopoietic stem cell transplantation abrogated donor HSC engraftment and was associated with strikingly flattened endosteal osteoblasts with preserved osteoblast proliferation and megakaryocyte migration. Depletion of monocytes, macrophages, or megakaryocytes (the predominant hematopoietic cell populations that survive short-term after irradiation) did not lead to an alteration of osteoblast morphology, suggesting that a hematopoietic-derived cell outside these lineages regulates osteoblast morphologic adaptation after irradiation. Using 2 lineage-tracing strategies, we identified a novel CD45^{-}F4/80^{lo} HSC-derived cell that resides among osteoblasts along the endosteal marrow surface and, at least transiently, survives radioablation. This newly identified marrow cell may be an important regulator of HSC engraftment, possibly by influencing the shape and function of endosteal osteoblasts.

Introduction

Hematopoietic stem cells (HSCs) reside in specialized microenvironments within the marrow that are designated stem cell niches. At homeostasis, the niche functions to maintain HSC quiescence, proliferation, and fate allocation, and after hematopoietic stem cell transplant (HCT) conditioning, it facilitates donor HSC engraftment, survival, and proliferation.[1] Hastening engraftment and hematopoietic reconstitution would represent a major advance in clinical HCT; however, such research is contingent upon a more complete understanding of the biology of the postablation niche, which is clearly distinct from niche biology during homeostasis.

The exact location and constituents of the hematopoietic niche have been widely explored and debated over the past few decades. Although our understanding of the hematopoietic niche continues to evolve, our current view is that at homeostasis, the marrow stem cell niche comprises many cell types and signals, including the arteriolar niche and the sinusoidal-megakaryocyte niche.[1-3] Osteolineage cells are

Submitted 5 June 2017; accepted 9 November 2017. DOI 10.1182/bloodadvances.2017008730.

The full-text version of this article contains a data supplement.

© 2017 by The American Society of Hematology

Downloaded from http://ashpublications.net/bloodadvances/article-pdf/1/27/2667/879379/advances008730.pdf by guest on 18 May 2024

a constituent of both niches[4-6]; however, the precise role of mature osteoblasts in HSC maintenance remains controversial. Adipocytes have also been investigated for their role in hematopoiesis, although their role is unclear at this time.[7,8]

The adaptive potential of these cellular microenvironments to respond to both pathological and physiological changes highlights the complex and vital interactions of the cellular constituents of the niche as well the important differences between homeostasis and postablated marrow niches. Successful hematopoietic reconstitution of donor HSC after HCT is dependent on a number of intricate cellular interactions, including recovery of the sinusoidal endothelium,[1,9-11] migration of megakaryocytes to the endosteal space, and osteoblast proliferation.[12] The role played by megakaryocytes in this niche is evidence of this adaptation because megakaryocytes function to promote quiescence via CXCL4[13] and TGF-β[14] at homeostasis and support HSC proliferation by secretion of fibroblast growth factor 1 (FGF1)[2] after HCT.[2,11,13] In addition, osteolineage cells may play a greater role in this adaptation than previously believed because primitive hematopoietic cells seem to initially localize to the osteoblast surface after HCT,[15,16] underscoring the importance of osteoblasts in the postablated marrow niche.

Here, we report that in situ targeted depletion of hematopoietic cells immediately before marrow radioablation abrogated donor HSC engraftment after HCT and was associated with strikingly flattened endosteal osteoblasts that failed to undergo normal conformational changes induced by radioablation. By using 2 lineage-tracing strategies, we identified a novel $CD45^{-}F4/80^{lo}$ HSC-derived cell that resides among osteoblasts along the endosteal marrow surface and, at least transiently, survives radioablation. This newly identified marrow cell may be an important regulator of HSC engraftment, possibly by directing adaptations of the endosteal osteoblasts to myeloablative HCT conditioning.

Materials and methods

Mice and irradiation

Experiments were conducted in accordance with protocols approved by Institutional Animal Care and Use Committee, and colonies were housed and maintained in the vivarium at The Research Institute at Nationwide Children's Hospital. All mice were purchased from The Jackson Laboratory with the exception of the CD45Cre strain that was originally obtained from Eva Mezey, MD (National Institutes of Health).[17] The Cre/loxP system[18] was used to generate double transgenic F1 mice expressing the inducible diphtheria toxin receptor (iDTR) in specific Cre-expressing cell targets as described by Buch et al[19] or in Z/RED[20] or Ai9[21] mice in lineage-tracing models. Triple transgenic F2 mice were developed by crossing cell-specific Cre/iDTR, cell-specific Cre/Z/RED, or Ai9 F1 mice with the Col2.3GFP strain[22] (for all mouse strains, see supplemental Table 1). Mice ranged in age from 6 to 18 weeks at the start of experiments. Total body irradiation (TBI) was performed by using a radiograph source (X-RAD 320, Precision X-ray Inc.). Five or more mice were used for all experiments unless otherwise specified.

In vivo cell depletion

Bone marrow hematopoietic cells were depleted in double-transgenic mice expressing iDTR on CD45-[17] or Vav1-expressing[23] cells. Mice received 100 ng of diphtheria toxin (DT) intraperitoneally 24 hours before TBI (1000 cGy) and were analyzed 48 hours after irradiation. Monocytes, macrophages, or megakaryocytes were depleted in transgenic mice expressing iDTR on lysozyme2-expressing (LYZ-Cre)[24] or PF4-expressing cells,[25,26] respectively. Mice received daily intraperitoneal injections of DT (100 ng) for 6 days, received TBI on day 4 (1000 cGy), and were analyzed 48 hours after irradiation. Chemical depletion of monocytes and macrophages[27] was accomplished by tail vein injection of clodronate (500 ng/day) for 5 days and TBI on day 4. All depletion models were monitored by peripheral blood counts on a Hemavet (Drew Scientific Inc.), and bone marrow (BM) was analyzed by flow cytometry and histology at 48 hours after irradiation. C57BL/6 mice and wild-type (WT) littermates were assessed in parallel as controls.

Histology studies

Mouse bones were fixed, decalcified, and paraffin embedded as previously described.[12,28] Briefly, femora and tibiae were fixed in either 10% neutral buffered formalin or 4% paraformaldehyde for 48 hours. Bones were then decalcified with either Regular Cal Immuno (BBC Biochemical, Mount Vernon, WA) for 5 to 7 days or 15% EDTA for 3 weeks before dehydration and paraffin embedding. Histologic sections were evaluated on an AxioImager 200M (Carl Zeiss, Thornwood, NY) or Zeiss 510 confocal microscope (Carl Zeiss) using 63×/1.4NA oil, 20×/0.5NA dry, and 40×/0.75NA dry objectives. Photographs were obtained with an Axiocam HRc or MRm camera and evaluated by using AxioVision 4.5SP1 software.

High-power fields (HPFs [20×]) of metaphyseal BM were examined, and the thickness of bone-lining cells was measured from at least 6 sections from each animal ($n \geq 5$.) For assessment of osteoblast proliferation, the osteoblast score index was evaluated, as described by Caselli et al,[28] which represents the average number of endosteal lining cell layers per section. The mean of 5 sections was taken as the individual mouse score. CD41-stained sections of metaphyseal BM were analyzed for total number and location of megakaryocytes at either the endosteal surface (within 1 cell diameter) or within the marrow space. At least 4 HPFs per section and more than 2 sections per mouse were averaged ($n > 4$ mice per group). Histologic assessment of cell-specific depletion was accomplished by immunohistochemistry (IHC) and/or immunofluorescence (IF) (see supplemental Data).

Secondary transplantation assay

A competitive secondary transplantation assay was performed as previously described by Olson et al.[12] Briefly, primary recipient CD45Cre or WT littermates underwent DT depletion (100 ng/day) followed by TBI (1000 cGY in split dosing). Mice were transplanted 48 hours later with 400 000 BM cells from H2K-GFP donor mice via tail vein injection. Thirty hours after transplant, BM was collected from primary recipients ($n = 5$ per cohort), pooled, and injected into irradiated WT secondary recipient mice ($n = 15$) along with 200 000 nonirradiated WT BM cells. Secondary recipients were assessed by peripheral blood analysis at 3, 8, and 16 weeks for percentages of green fluorescent protein (GFP)–expressing cells. BM analysis for the presence of GFP positivity was performed at 16 weeks to evaluate the effectiveness of primary recipient long-term HSC (LT-HSC) engraftment defined as >1% GFP.[12]

Downloaded from http://ashpublications.net/bloodadvances/article-pdf/1/27/2667/879379/advances008730.pdf by guest on 18 May 2024

Flow cytometric measurements

Flow cytometry analysis was performed on BD FACSCalibur and BD LSRII (BD Biosciences, San Jose, CA) cytometers using commercially available antibodies (BD Biosciences). Lineage (Lin) staining included anti-mouse TER119, GR1, B220, CD4 (RM4-5), CD8 (53-6.7), and CD11b (M1/70). Data were analyzed by using FlowJo version 10.0.6 software (Tree Star, Inc.). For flow cytometric analysis of bone-lining cells, marrow was vigorously flushed from the marrow space into fluorescence-activated cell sorting buffer. Bones were digested with collagenase P, and all washings were added to the collected marrow.

Statistical analysis

Statistical analyses were performed by using either unpaired two-tailed Student *t* test or one-way analysis of variance with multiple comparisons on Prism Version 6 (GraphPad Software Inc., La Jolla, CA). A minimum of 3 replicates were used for statistical analyses for each experiment. All statistical data are shown with mean ± standard error of the mean. $P < .05$ was considered statistically significant.

Results

In situ depletion of host hematopoietic cells before HSC transplant results in decreased donor HSC engraftment

To examine the effect of hematopoietic cell regulation of marrow remodeling and engraftment, we bred mice expressing Cre recombinase under the control of the CD45 promoter (CD45Cre) with iDTR transgenic mice to generate mice with DTR expression on hematopoietic cells. Importantly, all cells derived from CD45-expressing precursors, such as megakaryocytes, express DTR and can be selectively depleted, even if the mature cell lacks CD45 expression. To first validate the fidelity of the CD45Cre construct, we bred these mice to express a red fluorescent protein (RFP) reporter. Flow cytometric analysis of the CD45Cre/Z/RED mice showed RFP expression in 93% of the $CD45^+$ population in peripheral blood and in 91% of the $CD45^+$ population in BM.[29] We did not identify RFP expression in other tissues. We then generated CD45-driven DTR-expressing mice and used their $CD45Cre^-$ littermates as negative controls. Treatment with a single dose of 100 ng of DT yielded an 85% depletion of the leukocytes ($CD45Cre^+$, 0.56 ± 0.17 × 10^9/L; Cre^-, 6.59 ± 1.89 × 10^9/L; $P = .0053$) and 65% depletion of the platelets ($CD45Cre^+$, 769 ± 217 × 10^9/L; Cre^-, 283 ± 137 × 10^9/L; $P = .0304$) (Figure 1A), validating our in situ depletion model.

When mice underwent DT-mediated depletion of CD45-expressing cells followed by conventional radioablation and transplantation with normal marrow, all animals died before hematopoietic reconstitution. Because relatively few primitive hematopoietic cells are required to repopulate the marrow,[30] this observation suggested that the DT depletion created a defect in the host marrow microenvironment that diminished receptivity for transplanted HSCs.

We sought to determine whether the underlying failure of hematopoietic reconstitution in the CD45-depleted primary recipients is a modification of the donor LT-HSC ability to home and adhere within the marrow space or survive and proliferate within the niche once established in the marrow space. To distinguish between these 2 mechanisms, we assessed initial engraftment of long-term hematopoietic repopulating cells by using our semiquantitative competitive secondary transplantation assay[12] (Figure 1B), which tests for initial engraftment of LT-HSCs in the primary recipients. Surprisingly, only 1 of 15 of the secondary recipients of CD45-depleted primary mice had LT-HSC engraftment defined by >1% GFP expression compared with 10 of 15 control mice ($P = .0017$) (Figure 1C), confirming a striking deficit of initial HSC homing and adherence in the DT-depleted primary recipients.

Osteoblast flattening associated with in situ depletion of hematopoietic cells

At homeostasis, the endosteal surface is lined with a single layer of cuboidal osteoblasts and well-defined endothelial cells forming the marrow vasculature. Marrow megakaryocytes reside near the vasculature with only 8.60% ± 0.17% proximate to the endosteal surface (supplemental Figure 1A). In contrast, 48 hours after hematopoietic radioablation, the endosteal lining osteoblasts have proliferated to 2.64 ± 0.08 layers ($P < .0001$) and thickened from a baseline of 4.60 ± 0.23 μm to 8.17 ± 0.16 μm ($P < .0001$) (Figure 2A-B; supplemental Figure 1B-C). The vasculature was not clearly defined, and 40.70% ± 0.31% of the remaining megakaryocytes had migrated to the endosteal region, all consistent with our previous observations.[12,28,31]

Histologic assessment of femurs from mice treated with DT and TBI revealed proliferative, but significantly flattened osteoblasts (cell thickness, 3.42 ± 0.10 μm) in iDTR-expressing mice compared with similarly treated littermate controls (cell thickness, 8.45 ± 0.31 μm; $P < .0001$; Figure 2A-B), suggesting that depletion of host hematopoietic lineages is associated with the regulation of osteoblast morphology as well as donor HSC engraftment. Interestingly, osteoblast thickness in iDTR mice treated with DT only (no TBI) was significantly decreased compared with that in WT controls treated with DT (cell thickness, 2.89 ± 0.13 μm in iDTR mice vs 4.60 ± 0.23 μm in controls; Figure 2B). The total number of megakaryocytes in treated mice were significantly decreased compared with that in control mice (3.33 ± 0.54 cells per HPF in the CD45-depleted cohort vs 7.07 ± 0.60 cells per HPF in Cre^- littermates; $P = .0001$). However, of the remaining megakaryocytes, 33.3% ± 1.3% migrated to the endosteal surface, suggesting that the migratory capacity of megakaryocytes surviving the DT-mediated in situ depletion remained intact. Finally, assessment of BM morphology after myeloablative busulfan and cyclophosphamide (without TBI) was comparable to that seen after myeloablative TBI used in these experiments (T.S.O. and E.M.H., unpublished observation); thus, our results are not dependent on radioablation.

To confirm these findings, we repeated these experiments using an alternative double transgenic mouse that expressed Cre under the control of the Vav1 promoter (Vav1Cre) crossed with iDTR. Flow cytometric analysis of BM from Vav1Cre mice crossed with the RFP reporter mice showed 86.9% ± 7.8% of DsRed positivity within the CD45 population. Forty-eight hours after TBI of DT-treated DTR-expressing mice and their control littermates, histologic analysis showed that osteoblast morphology was again significantly flattened (4.55 ± 0.08 μm) compared with that of irradiated littermate controls (7.16 ± 0.43 μm; $P < .0001$), similar to our findings using the CD45Cre model (Figure 2C-D). Consistent results using 2 different transgenic promoters driving Cre

Downloaded from http://ashpublications.net/bloodadvances/article-pdf/1/27/2667/879379/advances008730.pdf by guest on 18 May 2024

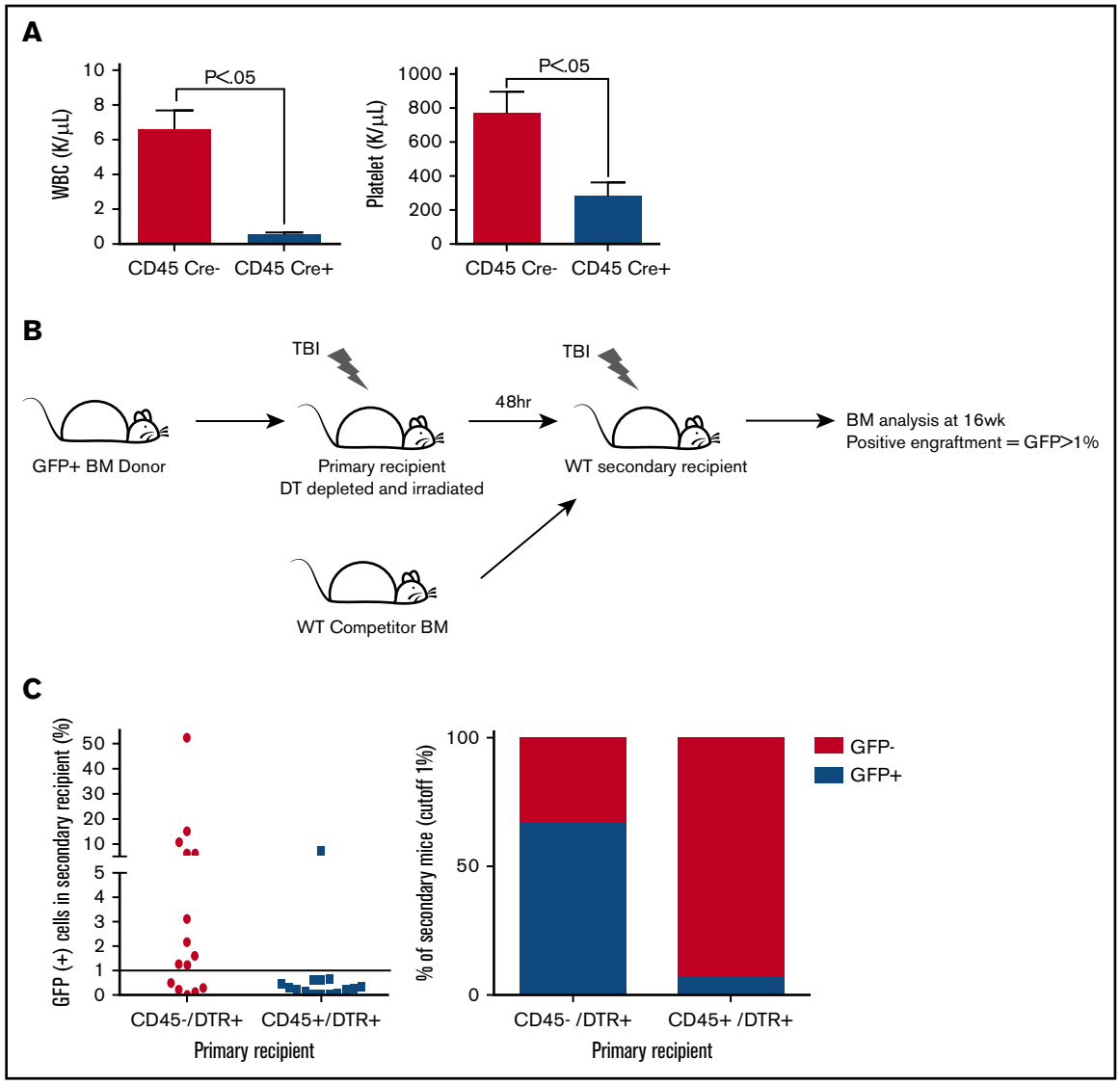

Figure 1. LT-HSC engraftment after BM transplantation is significantly impaired after hematopoietic cell depletion. (A) Peripheral blood analysis 48 hours after a single injection of 100 ng DT showed a significant depletion of leukocytes and platelets. (B) Pictogram describing a secondary transplant assay that used a GFP$^+$ BM donation to DT-depleted and irradiated primary recipients. Primary BM was then transplanted along with WT competitor BM into irradiated WT secondary recipients. Bone marrow analysis for the presence of GFP positivity was performed at 16 weeks to evaluate the effectiveness of primary recipient LT-HSC engraftment defined as >1% GFP. (C) Flow cytometric analysis of mouse BM 16 weeks after secondary transplant assay evaluating the LT-HSC engraftment. WBC, white blood cell count.

expression suggested that a model-independent regulatory mechanism involving cells derived from hematopoietic lineages is responsible for driving osteoblast morphologic changes that correlate with successful HSC engraftment after HCT.

Because earlier studies have shown the importance of osteoblast size and shape for both hematopoiesis[32] and retention or egress of HSCs from the BM,[33,34] we sought to determine how closely radioablation-induced changes in osteoblast thickness can serve as an index for the niche capacity to engraft donor HSCs. Our data implicate host CD45-expressing cells that persist after radioablation as regulatory components of this morphologic adaptation. Megakaryocytes (which are known to remain functional in murine models 7 to 10 days after irradiation[31]) and monocytes and macrophages that survive short-term after irradiation[33] were our most likely candidates. Analyses of WT mice 48 hours after irradiation confirmed the survival of these 2 dominate hematopoietic populations in BM.[31]

In situ depletion of monocytes and macrophages does not alter post-TBI osteoblast morphology

To evaluate the role of monocytes and macrophages on osteoblast enlargement, we depleted these cells in situ using 2 models. First, we generated mice expressing DTR directed by the lysozyme promoter LYZ/iDTR, which predominately but not exclusively labels monocytes and macrophages. Second, we used a pharmacologic depletion with clodronate, given recent studies that showed varying results between the 2 depletion methods.[33] Flow cytometric analysis (Figure 3A) of the CD11b BM population decreased from an average

Downloaded from http://ashpublications.net/bloodadvances/article-pdf/1/27/2667/879379/advances008730.pdf by guest on 18 May 2024

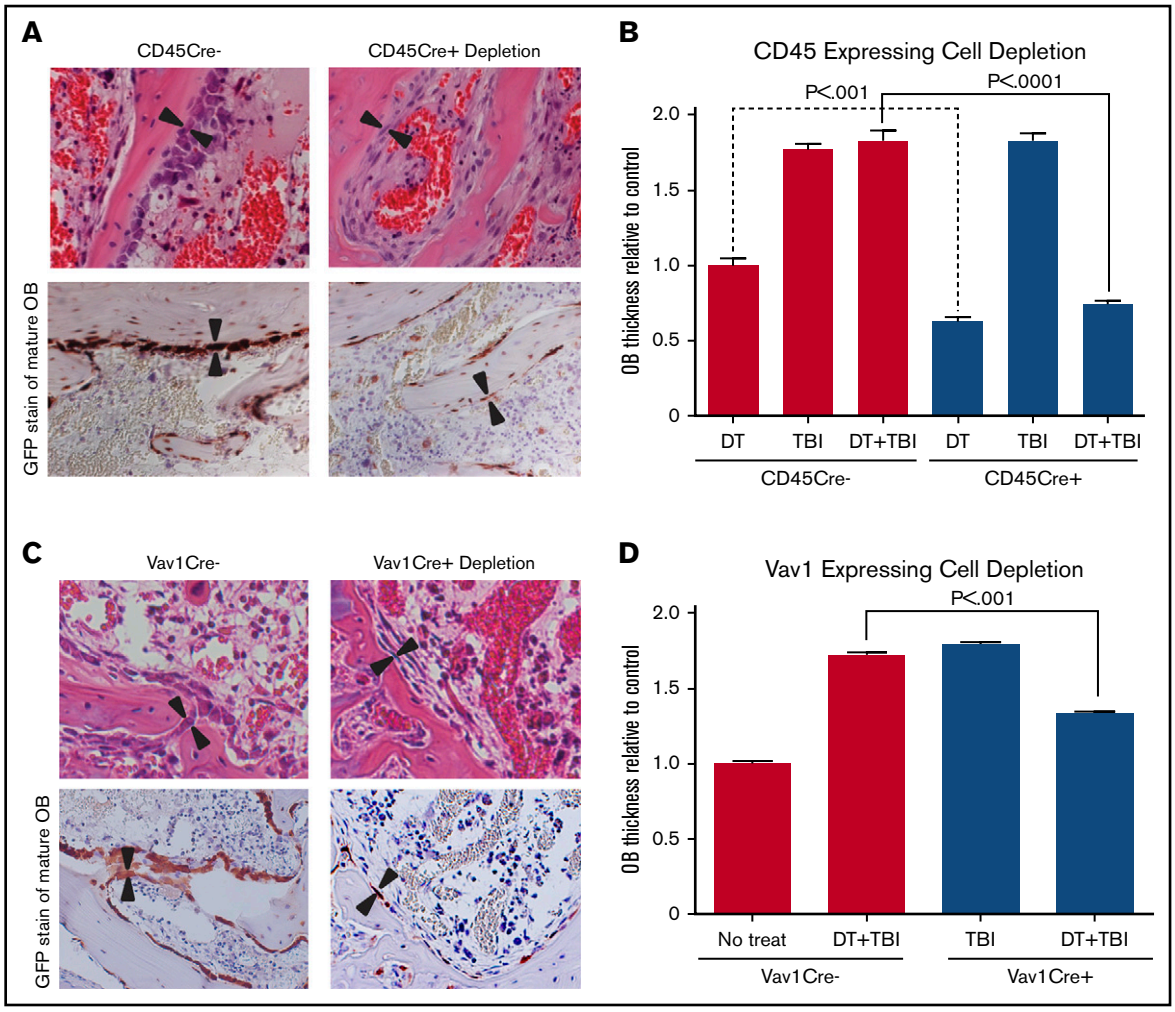

Figure 2. BM remodeling and osteoblast morphology after hematopoietic cell depletion and TBI. (A) Hematoxylin and eosin (H&E)–stained and GFP-stained sections (40×) of metaphyseal BM 48 hours after both DT depletion and TBI in CD45Cre$^-$ (control) and CD45Cre$^+$-depleted mice demonstrating depletion of hematopoietic cells and alterations in osteoblast (OB) thickness. (B) Quantitative analysis of osteoblast thickness (n ≥ 5) after DT injection only, TBI only, or DT injection and TBI in mice expressing iDTR with and without the presence of CD45Cre cells. Results show a significant decrease in osteoblast thickness (3.42 ± 0.11 μm vs WT, 8.45 ± 0.31 μm; $P < .0001$) between mice treated with DT and TBI in the CD45Cre$^+$ cohort. There was also a significant decrease between CD45Cre$^-$ and CD45Cre$^+$ mice treated with DT injection only (4.60 ± 0.23 μm in CD45Cre$^-$ vs 2.89 ± 0.13 μm in CD45Cre$^+$; $P < .0001$). (C) H&E-stained and GFP-stained sections (40×) of metaphyseal BM 48 hours after DT injection and TBI in Vav1Cre$^-$ (control) and Vav1Cre$^+$-depleted mice (n ≥ 5). (D) Analysis of osteoblast thickness in Vav1 depletion model confirming osteoblast flattening (4.55 ± 0.08 μm vs WT, 7.16 ± 0.43 μm; $P < .0001$).

of 13.86% ± 2.41% to 3.15% ± 0.58% in the LYZ/iDTR cohort, which represents an 80% depletion ($P = .003$) and 24.9% ± 2.45% to 10.6% ± 2.26% in the clodronate cohort ($P = .005$) in irradiated mice. Analysis of the F4/80 BM populations in the LYZ/iDTR cohort showed 75% depletion, with a decrease from 1.70% ± 0.30% to 0.38% ± 0.70% ($P = .008$), and the clodronate cohort showed a decrease from 2.37% ± .44% to 0.96% ± .07% ($P = .015$) in irradiated mice.

Osteoblast enlargement was preserved with both depletion methods compared with that in untreated littermate controls (cell thickness, 7.35 ± 0.76 μm vs 3.16 ± 0.57 μm [$P < .0001$] in the LYZ cohort and 6.44 ± 0.84 μm vs 3.16 ± 0.57 μm [$P < .0001$] in the clodronate cohort) and DT- treated and irradiated control group (cell thickness, 7.35 ± 0.76 μm vs 7.16 ± 0.43 μm [P = ns] in the LYZ cohort and 6.44 ± 0.84 μm vs 6.84 ± 0.42 μm [P = ns] in the clodronate cohort) (Figure 3B-C). Although we did not obtain complete depletion with either model, we used 2 very different depletion strategies to most thoroughly assess for a monocyte or macrophage contribution. Our data suggest that classic monocytes and macrophages are not responsible for morphologic changes of endosteal osteoblasts.

In situ depletion of megakaryocytes does not alter post-TBI osteoblast morphology

The megakaryocyte population was then evaluated as the osteoblast regulatory population because megakaryocytes have been shown to remain functional for 7 to 10 days after irradiation and extensively interact with the endosteal bone.[31,35] Megakaryocytes were depleted in PF4Cre/iDTR mice with DT injections, and mean platelet counts decreased by 85% compared with those in DT-treated littermate

Downloaded from http://ashpublications.net/bloodadvances/article-pdf/1/27/2667/879379/advances008730.pdf by guest on 18 May 2024

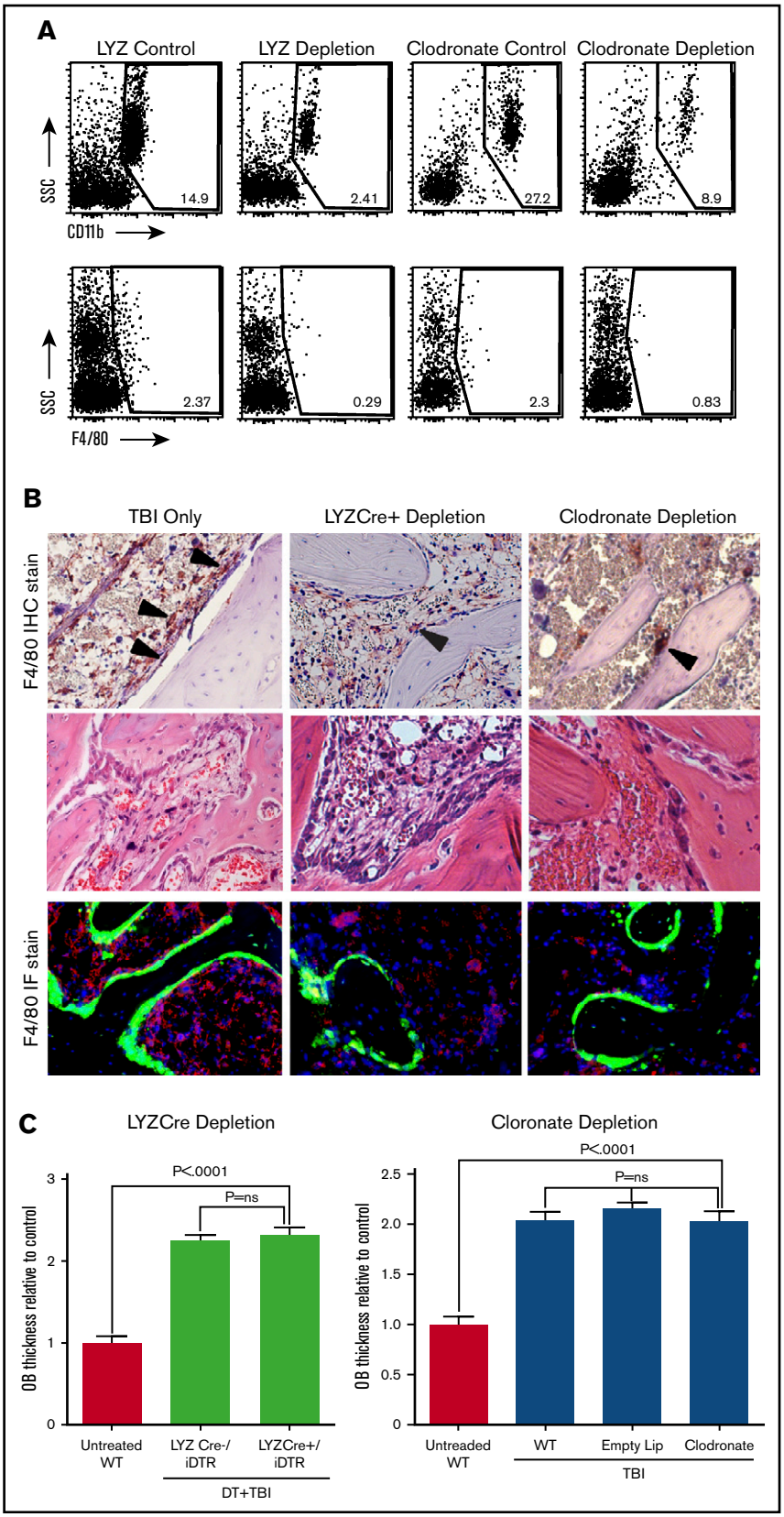

Figure 3. Effect of monocyte/macrophage depletion on osteoblast thickness. (A) Flow analysis of BM after DT or clodronate depletion at 48 hours after TBI showing depletion of F4/80 and CD11b cell populations. (B) BM sections (40×) of DT depleted, clodronate depleted, and WT control 48 hours after TBI stained for F4/80 showing histologic depletion of osteomacrophages in all groups (top). H&E-stained sections (40×) of metaphyseal BM showing consistent thickness of osteoblasts despite depletion (middle.) IF-stained section of metaphyseal BM (40× objective) showing depletion of F4/80 population (red) with reservation of osteoblast thickening (green) in all groups (bottom). (C) Histologic analysis of osteoblast thickness in LYZ/iDTR and clodronate depletion show no significant change from TBI only group (LYZ/iDTR cohort cell thickness, 7.35 ± 0.76 μm vs 7.16 ± 0.43 μm; P = not significant [ns]; clodronate cohort cell thickness, 6.44 ± 0.85 μm vs 6.44 ± 0.85 μm; P = ns). SSC, side scatter channel.

Downloaded from http://ashpublications.net/bloodadvances/article-pdf/1/27/2667/879379/advances008730.pdf by guest on 18 May 2024

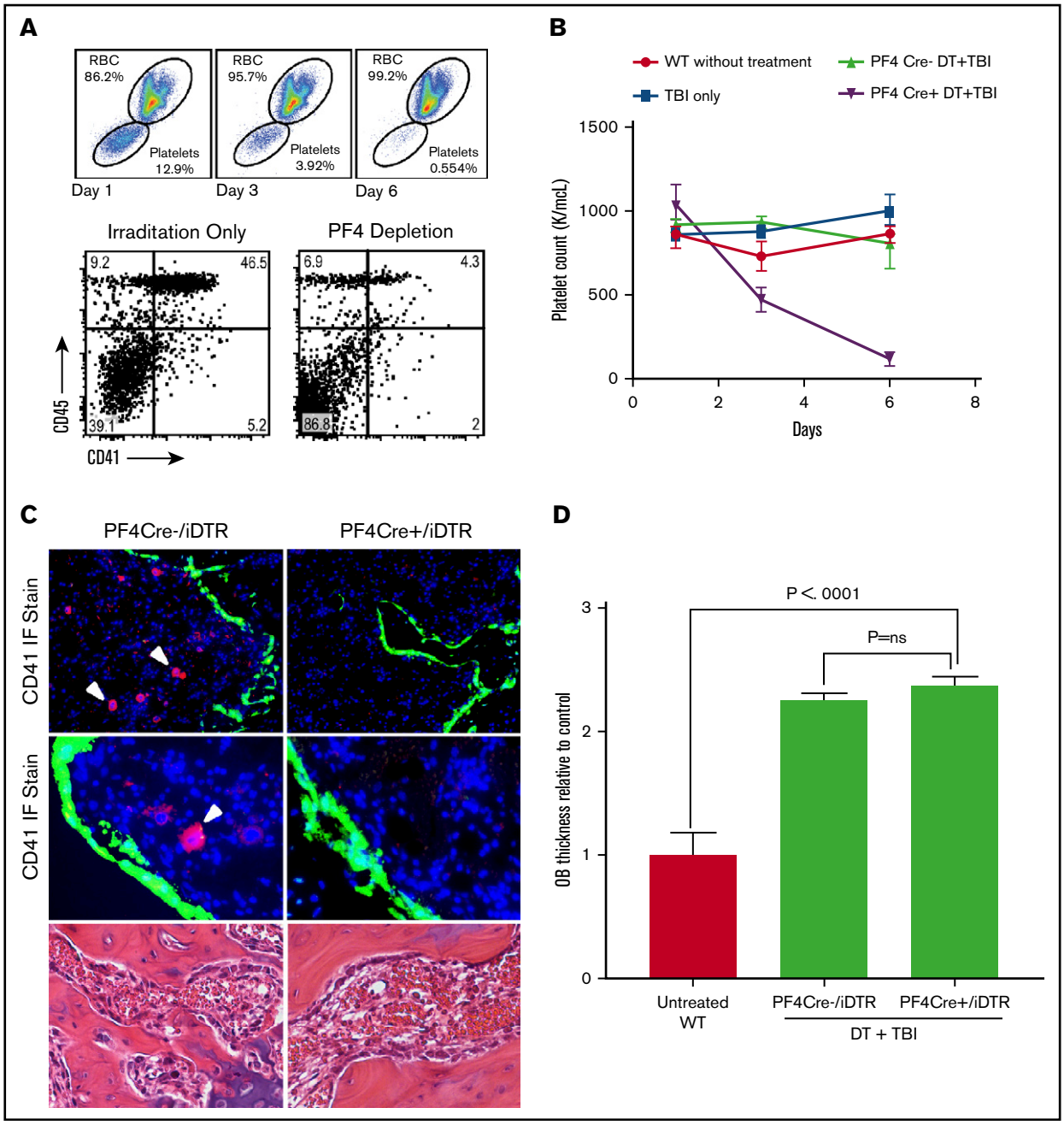

Figure 4. Effect of megakaryocyte depletion on osteoblast thickening. (A) Flow cytometric analysis of peripheral blood at days 0, 3, and 6 of DT injections showing depletion of peripheral platelets (top) and flow cytometric analysis of BM from PF4/iDTR mouse after 5-day treatment with DT and 48 hours after irradiation showing depletion of $CD41^+$ cells (below). (B) Mean platelet counts decreased by 85% compared with DT-treated controls. (C) IF-stained sections (20× top; 40× middle) of BM metaphysis showing significant CD41 (red) depletion and thickening of GFP (green)-labeled osteoblasts in PF4/iDTR × Col2.3GFP triple transgenic mice and $PF4Cre^-$ controls treated with DT and 48 hours after irradiation. H&E-stained sections (40× bottom) of PF4/iDTR and $PF4Cre^-$ control mice demonstrating similar osteoblast thickening. (D) Analysis of osteoblast thickness in PF4Cre DT depletion compared with $PF4Cre^-$ controls shows increased osteoblast thickness compared with irradiated controls (cell thickness, 7.51 ± 0.62 μm vs 7.16 ± 0.43 μm; P = ns). RBC, red blood cell.

controls (n ≥ 6) (PF4/iDTR, 116.9 ± 42.6 × 10^9/L; treated controls, 808.6 ± 153 × 10^9/L; P = .0007) (Figure 4B). Flow cytometry confirmed an 83% depletion of $CD41^+$ cells, with the population decreasing from 32.2% ± 5.7% to 5.69% ± 1.70% (P = .002) (Figure 4A). IF and IHC evaluation visually confirmed a significant reduction of the $CD41^+$ cell population in PF4/iDTR mice compared with WT littermates (2.8 ± 0.3 cells vs 7.07 ± 0.61 cells; P = .0005) (Figure 4C).

Analysis of postirradiation osteoblast thickness after megakaryocyte depletion revealed a statistically significant increase in osteoblast thickness compared with that in untreated controls (cell thickness, 7.51 ± 0.62 μm vs 3.16 ± 0.57 μm; P < .0001)

Downloaded from http://ashpublications.net/bloodadvances/article-pdf/1/27/2667/879379/advances008730.pdf by guest on 18 May 2024

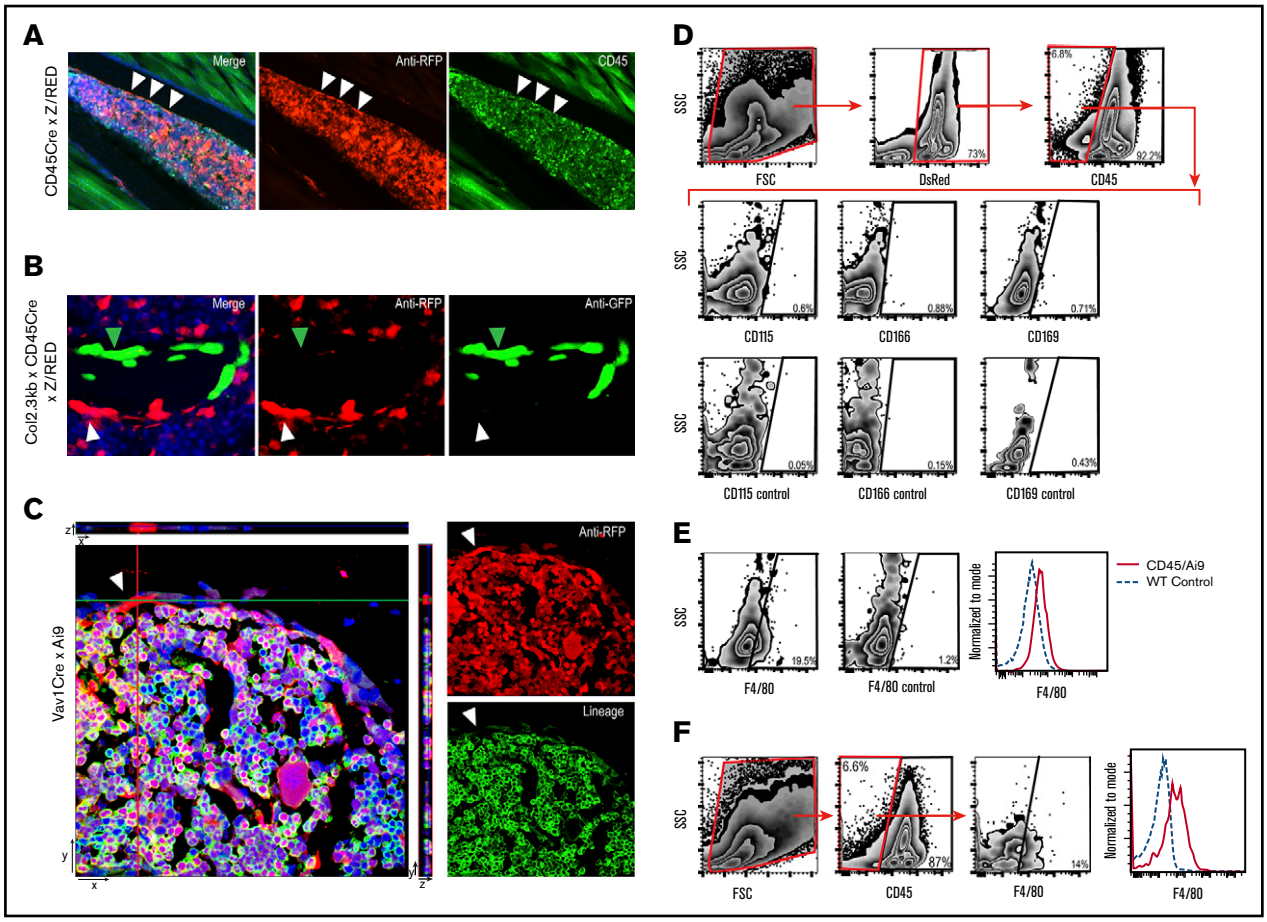

Figure 5. CD45Cre-labeled murine BM. (A) IF-stained metaphyseal bone sections (20×) of RFP-labeled CD45Cre mouse showing BM at homeostasis. White arrows indicate a red CD45-derived cell that resides near the endosteal region. Green CD45 stain reveals that the cell no longer expresses CD45. (B) IF metaphyseal section (40×) of BM from DsRed-labeled CD45Cre mouse crossed with a Col2.3GFP mouse, which GFP labels mature osteoblast. White arrowhead indicates the red CD45-derived cell; green arrowhead indicates the GFP-labeled mature osteoblast. (C) Confocal Z-stack image (63×) showing RFP Vav1-derived cell that does not stain for lineage markers (B220, CD3, Ter119, Gr1, CD11b). (D) Flow cytometric analysis of transgenic CD45/Ai9 mouse BM and bone-lining cells gated on $DsRed^+/CD45^-$ population. (E) Dot plot and histogram depiction of transgenic CD45/Ai9 mouse BM and bone-lining cells gated on $DsRed^+/CD45^-$ population showing shift of F4/80 expression. F4/80 expression on dot plot showed an average of 17.27% ± 3.6% positivity vs 1.1% ± 0.015% in unstained controls. (F) Flow cytometric analysis of WT mouse BM and bone-lining cells gated on $CD45^-$ population. F4/80 expression on dot plot analysis showed an average of 13.5% ± 0.8% positivity vs 1.1% ± 0.015% in unstained controls.

and in the DT-treated and irradiated control group (cell thickness, 7.51 ± 0.62 μm vs 7.16 ± 0.43 μm; P = ns) (Figure 4C-D). Although the number of megakaryocytes significantly decreased (2.96 ± 0.82 cells per HPF vs 7.10 ± 1.43 cells in controls per HPF), megakaryocyte migration (~40% of the remaining cells) was consistent with that in irradiated WT mice, which may in part underlie the unimpaired osteoblast proliferation. These data suggests that although megakaryocytes are important for osteoblast proliferation, they do not drive the osteoblast morphologic change seen in our CD45-lineage depletion model.

Identification of a novel $CD45^-F4/80^{lo}$ bone-lining cell as a candidate regulatory element

To identify other candidates for the osteoblast morphology regulatory cells, we used 2 lineage-tracing strategies (CD45- and Vav1-directed RFP) to reveal hematopoietic cells that survive, at least short-term, after radioablation. Surprisingly, we identified a novel cell residing in the bone marrow among endosteal osteoblasts that was developmentally derived from a hematopoietic progenitor (as identified by the RFP lineage reporter) but lacked CD45 expression (Figure 5A). When CD45/Z/RED mice were crossed with Col2.3GFP transgenic mice (which express GFP in mature osteoblasts[22]), RFP-expressing bone-lining cells lacked GFP co-expression by IHC staining (Figure 5B) and flow cytometry,[29] indicating they are not mature osteoblasts.

By using confocal microscopy with IF staining, we determined that these $CD45^-RFP^+$ cells lacked expression of lineage markers (including Gr1, CD11b, CD3, B220, Ter119; Figure 5C) and cathepsin K,[29] indicating they are not conventional hematopoietic cells, specifically not osteoclasts; nonetheless, they were derived from CD45-expressing progenitors (Figure 5B). With confocal microscopy, we visualized individual $CD45^-Lin^-RFP^+$ cells along the endosteum, confirming the identification of a novel hematopoietic lineage–derived (RFP expression) bone-lining cell (Figure 5C).

Downloaded from http://ashpublications.net/bloodadvances/article-pdf/1/27/2667/879379/advances008730.pdf by guest on 18 May 2024

Flow cytometric characterization of freshly isolated $CD45^{-}RFP^{+}$ cells confirmed that these cells lacked most hematopoietic antigens but revealed F4/80 expression (Figure 5D). Compared with conventional $CD45^{+}F4/80^{+}$ monocytes, F4/80 expression was low but unequivocal, most likely indicating low expression on a relatively small population in the marrow microenvironment (Figure 5E). Conceivably, lineage tracing may have revealed a heterogeneous population of RFP^{+} cells with a continuum of detectable F4/80 expression. Although F4/80 expression is considered to be a marker of the monocyte/macrophage family in mice, these cells lacked expression of other monocyte/macrophage surface markers such as CD11b, CD115, CD14, CD166, and CD169 (Figure 5D) as well as the leukocyte marker CD45. Collectively, our data suggest that the phenotype $CD45^{-}F4/80^{lo}$ specifically identifies this novel hematopoietic-derived bone-lining cell.

Because DT depletion of CD45-derived cells just before hematopoietic radioablation leads to poor donor HSC engraftment and flattened osteoblasts, a morphology not observed with depletion of classically defined monocytes and macrophages or megakaryocytes, we postulated that the $CD45^{-}F4/80^{lo}RFP^{+}$ cell is a candidate regulatory cell for endosteal osteoblast function. Consistent with this notion, the frequency of $CD45^{-}RFP^{+}$ cells is greater in the metaphysis (the site of initial donor HSC engraftment[31,36]) compared with the diaphysis, and these cells expand similarly to endosteal osteoblasts after marrow radioablation. Most intriguing, $CD45^{-}F4/80^{lo}RFP^{+}$ cells seem to express nestin by reverse transcription polymerase chain reaction (supplemental Figure 2) but do not differentiate to osteoblasts in vitro. This is consistent with other cellular constituents of marrow niches but not mesenchymal stem-like cells.[37] Given that osteoblasts have been shown to flatten after several days of granulocyte colony-stimulating factor (G-CSF) exposure,[34,38,39] we explored the possible role of G-CSF on our cell population. However, flow cytometric evaluation of a G-CSF receptor did not demonstrate expression. Finally, we identified a $CD45^{-}F4/80^{lo}$ population among the bone-lining cells in normal C57BL/6 mice without lineage tracing, affirming the existence of these unique cells (Figure 5F).

Discussion

Quite unexpectedly, we have unambiguously identified a novel hematopoietic-derived cell residing at the marrow endosteal surface that can be identified by the unique $CD45^{-}F4/80^{lo}$ phenotype. The striking correlation of our DT depletion data are consistent with $CD45^{-}F4/80^{lo}$ cells possibly being critical regulators of donor HSC engraftment through modulation of niche osteoblast morphology. These cells are distinct from the $CD115^{int}F4/80^{+}CD169^{+}$ macrophages described by Chow et al[40] that have been shown to be active in the retention of HSCs within the stem cell niche and the mesenchymal stem cells described by Mendez-Ferrer et al.[37] These cells seem to express nestin, which is consistent with adrenergic input affecting the regulatory functions.[41]

We have previously shown that marrow microenvironment remodeling in response to radioablation, which includes osteoblast enlargement, osteoblast proliferation, and megakaryocyte migration, is critical for efficient HSC engraftment.[12,28,31] We have shown herein that endosteal osteoblast morphology, which could be regulated by $CD45^{-}F4/80^{lo}$ cells, is an important attribute of postablation niche remodeling, which influences the ability of the niche to engraft donor HSCs. Cell morphology affects membrane biophysical properties and plays a role in adhesion of HSCs within the marrow space.[34,42] This notion is supported by studies showing that upon adrenergic stimulation from the nervous system, osteoblasts flatten and stiffen, thus altering their adhesiveness for HSCs and contributing to HSC mobilization from the marrow niche.[34,42] Indeed, that cell size and shape alter adhesion properties is a recurrent theme in developmental biology.[43,44] Endosteal osteoblast morphology may conceivably provide a marker for the regulatory cell impacts on marrow adaptations during HCT that foster HSC engraftment.

Given that host megakaryocytes are required for efficient HSC engraftment[12] and that hematopoietic depletion rids the marrow of approximately 80% of megakaryocytes, why is megakaryocyte depletion not the underlying explanation for the lack of observed engraftment? We previously reported that complete blockade of megakaryocyte migration with preservation of osteoblast enlargement and proliferation leads to diminished but not abolished HSC engraftment. The ~40% of remaining megakaryocytes that migrate to the proliferating, flattened osteoblasts would be expected to facilitate a low but measurable level of HSC engraftment.[12] However, we have shown in this study that donor engraftment was not detected, and therefore, megakaryocytes, although they are necessary for engraftment (as shown by our previous study), are not sufficient for engraftment in the absence of the appropriate osteoblast morphologic change. Collectively, our data suggest that although osteoblast proliferation and megakaryocyte migration are necessary for successful long-term engraftment,[12,28] osteoblast thickness may be critical for efficient HSC retention in the marrow after homing.

The finding of $F4/80^{lo}$ on this cell suggests that this cell derives from the monocyte/macrophage lineage; however, monocyte lineage depletion by DT and clodronate did not show a morphologic change within the marrow space. Moreover, the classic markers of monocytes and macrophages were not expressed by these cells. Given that we attained effective but not complete depletion with each model, this cell conceivably could be a macrophage variant that survived depletion in both models and has lost CD45 expression during its development. Further evaluation will help characterize this murine cell and identify potential targets for human study because the human homolog of F4/80 is the eosinophil-specific receptor EMR1.[45]

Finally, is the biology we have identified germane to patient care? HSC ablation by TBI has been the backbone of myeloablative HCT preparation for patients with recurrent acute leukemia as well as other BM diseases. Multiple reports have shown superior outcomes in event-free survival in patients with relapsed leukemia treated with TBI compared with those treated with myeloablative chemotherapy alone.[46-49] Assessment of the BM morphology after chemotherapy alone was evaluated, and the extent of endosteal cell expansion after myeloablative conditioning with busulfan and cyclophosphamide was comparable to that seen with myeloablative TBI. These findings suggests that our current results are due to hematopoietic ablation but not specifically TBI. Thus, we suggest that our observations are highly relevant to clinical HCT. Moreover, the use of TBI in this study allows for direct comparison with our previous work. Our future work will, in part, focus on approaches to leverage this biology to hasten the time to engraftment in the clinical setting.

Our data provide 3 key findings. First, we unambiguously identified a novel $CD45^{-}F4/80^{lo}$ cell that resides within the bone among the endosteal osteoblasts but is derived from hematopoietic

Downloaded from http://ashpublications.net/bloodadvances/article-pdf/1/27/2667/879379/advances008730.pdf by guest on 18 May 2024

progenitors. Second, in situ depletion of hematopoietic cells before conventional radioablation results in strikingly flattened endosteal osteoblasts. And third, targeted depletion of hematopoietic cells before radioablation generates a niche defect that abrogates donor HSC engraftment. Our conclusions rely heavily on DT/iDTR in situ depletion of hematopoietic cells using transgenic mice with tissue-specific Cre expression. The primary pitfall of this strategy is lineage infidelity of the promoter, which leads to the unintended depletion of cells other than those targeted. To mitigate the risk of unknowingly generating erroneous results, we used 2 different transgenic constructs that used 2 different hematopoietic-specific promoters. We were able to replicate our findings with both CD45- and Vav1-directed Cre expression, which underscores the rigor of our conclusions.

Future investigations will be aimed at identifying a unique global marker of our novel cell that will allow for selective depletion to further assess its role in the hematopoietic niche, HSC engraftment, and osteoblast morphology. With pan-CD45 depletion, we recognize the possibility that systemic inflammation above baseline may account for the engraftment defect; however, in our studies the mice did not display a phenotype consistent with a lethal systemic inflammatory reaction, and timing of death was most consistent with aplasia. Endothelium is disrupted with TBI, and supportive stromal elements such as mesenchymal stromal cells would not likely be affected by DT injection. In addition, the observed flattened osteoblast morphology cannot be readily explained by systemic inflammation. Although the mechanistic link between depletion of our novel cell and osteoblast morphology remains to be determined, previous studies performed by our group[12,28,31] and others[32,34,42] suggest an important role for osteoblast morphology in the retention of HSCs. Moreover, our newly identified $CD45^{-}F4/80^{lo}$ cell may prove to be an important constituent of the stem cell niche, even if it does not regulate osteoblast morphology.

Acknowledgments

The authors acknowledge Eva Mezey, National Institutes of Health, for providing founder mice for the CD45Cre colony, Ted J. Hofmann for technical work, and the Morphology Core, Flow Cytometry Core, and Animal Resources Core at Nationwide Children's Hospital for their resources and services.

Authorship

Contribution: K.M.O. helped design and perform all experiments, analyzed and interpreted the data, and prepared the manuscript; S.O. helped design and perform experiments, analyze data, and review the manuscript; T.S.O. interpreted the data and reviewed the manuscript; A.J.G. generated transgenic animals, performed experiments, and reviewed the manuscript; V.M.V. performed histologic experiments and interpreted flow cytometric experiments; L.D. performed and interpreted flow cytometric experiments; M.D. interpreted data and reviewed the manuscript; and E.M.H. oversaw the entire project, designed and analyzed the experiments, and edited and finalized the manuscript.

Conflict-of-interest disclosure: The authors declare no competing financial interests.

Correspondence: Edwin M. Horwitz, Center for Childhood Cancer and Blood Diseases, The Research Institute at Nationwide Children's Hospital, 700 Children's Dr, Columbus, OH 43205; e-mail: edwin.horwitz@nationwidechildrens.org.

References

1. Calvi LM, Link DC. The hematopoietic stem cell niche in homeostasis and disease. *Blood*. 2015;126(22):2443-2451.
2. Zhao M, Perry JM, Marshall H, et al. Megakaryocytes maintain homeostatic quiescence and promote post-injury regeneration of hematopoietic stem cells. *Nat Med*. 2014;20(11):1321-1326.
3. Nombela-Arrieta C, Pivarnik G, Winkel B, et al. Quantitative imaging of haematopoietic stem and progenitor cell localization and hypoxic status in the bone marrow microenvironment. *Nat Cell Biol*. 2013;15(5):533-543.
4. Zhang J, Niu C, Ye L, et al. Identification of the haematopoietic stem cell niche and control of the niche size. *Nature*. 2003;425(6960):836-841.
5. Calvi LM, Adams GB, Weibrecht KW, et al. Osteoblastic cells regulate the haematopoietic stem cell niche. *Nature*. 2003;425(6960):841-846.
6. Nakamura Y, Arai F, Iwasaki H, et al. Isolation and characterization of endosteal niche cell populations that regulate hematopoietic stem cells. *Blood*. 2013;116(9):1422-1432. .
7. Naveiras O, Nardi V, Wenzel PL, Hauschka PV, Fahey F, Daley GQ. Bone-marrow adipocytes as negative regulators of the haematopoietic microenvironment. *Nature*. 2009;460(7252):259-263.
8. Zhou BO, Yu H, Yue R, et al. Bone marrow adipocytes promote the regeneration of stem cells and haematopoiesis by secreting SCF. *Nat Cell Biol*. 2017;19(8):891-903.
9. Hoggatt J, Kfoury Y, Scadden DT. Hematopoietic stem cell niche in health and disease. *Annu Rev Pathol*. 2016;11(1):555-581.
10. Hooper AT, Butler JM, Nolan DJ, et al. Engraftment and reconstitution of hematopoiesis is dependent on VEGFR2-mediated regeneration of sinusoidal endothelial cells. *Cell Stem Cell*. 2009;4(3):263-274.
11. Birbrair A, Frenette PS. Niche heterogeneity in the bone marrow. *Ann N Y Acad Sci*. 2016;1370(1):82-96.
12. Olson TS, Caselli A, Otsuru S, et al. Megakaryocytes promote murine osteoblastic HSC niche expansion and stem cell engraftment after radioablative conditioning. *Blood*. 2013;121(26):5238-5249.
13. Bruns I, Lucas D, Pinho S, et al. Megakaryocytes regulate hematopoietic stem cell quiescence through CXCL4 secretion. *Nat Med*. 2014;20(11):1315-1320.
14. Söderberg SS, Karlsson G, Karlsson S. Complex and context dependent regulation of hematopoiesis by TGF-β superfamily signaling. *Ann N Y Acad Sci*. 2009;1176(1):55-69.

Downloaded from http://ashpublications.net/bloodadvances/article-pdf/1/27/2667/879379/advances008730.pdf by guest on 18 May 2024

15. Nilsson SK, Johnston HM, Coverdale JA. Spatial localization of transplanted hemopoietic stem cells: inferences for the localization of stem cell niches. 2001;97(8):2293-2299.

16. Xie Y, Yin T, Wiegraebe W, et al. Detection of functional haematopoietic stem cell niche using real-time imaging. *Nature*. 2009;457(7225):97-101.

17. Bratincsák A, Brownstein MJ, Cassiani-Ingoni R, et al. CD45-positive blood cells give rise to uterine epithelial cells in mice. *Stem Cells*. 2007;25(11): 2820-2826.

18. Branda CS, Dymecki SM. Talking about a revolution: The impact of site-specific recombinases on genetic analyses in mice. *Dev Cell*. 2004;6(1):7-28.

19. Buch T, Heppner FL, Tertilt C, et al. A Cre-inducible diphtheria toxin receptor mediates cell lineage ablation after toxin administration. *Nat Methods*. 2005; 2(6):419-426.

20. Vintersten K, Monetti C, Gertsenstein M, et al. Mouse in red: red fluorescent protein expression in mouse ES cells, embryos, and adult animals. *Genesis*. 2004;40(4):241-246.

21. Madisen L, Zwingman TA, Sunkin SM, et al. A robust and high-throughput Cre reporting and characterization system for the whole mouse brain. *Nat Neurosci*. 2010;13(1):133-140.

22. Kalajzic I, Kalajzic Z, Kaliterna M, et al. Use of type I collagen green fluorescent protein transgenes to identify subpopulations of cells at different stages of the osteoblast lineage. *J Bone Miner Res*. 2002;17(1):15-25.

23. de Boer J, Williams A, Skavdis G, et al. Transgenic mice with hematopoietic and lymphoid specific expression of Cre. *Eur J Immunol*. 2003;33(2): 314-325.

24. Clausen BE, Burkhardt C, Reith W, Renkawitz R, Förster I. Conditional gene targeting in macrophages and granulocytes using LysMcre mice. *Transgenic Res*. 1999;8(4):265-277.

25. Tiedt R, Schomber T, Hao-Shen H, Skoda RC. Pf4-Cre transgenic mice allow the generation of lineage-restricted gene knockouts for studying megakaryocyte and platelet function in vivo. *Blood*. 2007;109(4):1503-1506.

26. Wuescher LM, Takashima A, Worth RG. A novel conditional platelet depletion mouse model reveals the importance of platelets in protection against Staphylococcus aureus bacteremia. *J Thromb Haemost*. 2015;13(2):303-313.

27. van Rooijen N, Sanders A, van den Berg TK. Apoptosis of macrophages induced by liposome-mediated intracellular delivery of clodronate and propamidine. *J Immunol Methods*. 1996;193(1):93-99.

28. Caselli A, Olson TS, Otsuru S, et al. IGF-1-mediated osteoblastic niche expansion enhances long-term hematopoietic stem cell engraftment after murine bone marrow transplantation. *Stem Cells*. 2013;31(10):2193-2204.

29. Otsuru S, Overholt KM, Olson TS, et al. Hematopoietic derived cells do not contribute to osteogenesis as osteoblasts. *Bone*. 2017;94:1-9.

30. Kiel MJ, Yilmaz ÖH, Iwashita T, Yilmaz OH, Terhorst C, Morrison SJ. SLAM family receptors distinguish hematopoietic stem and progenitor cells and reveal endothelial niches for stem cells. *Cell*. 2005;121(7):1109-1121.

31. Dominici M, Rasini V, Bussolari R, et al. Restoration and reversible expansion of the osteoblastic hematopoietic stem cell niche after marrow radioablation. *Blood*. 2009;114(11):2333-2343.

32. Visnjic D, Kalajzic Z, Rowe DW, Katavic V, Lorenzo J, Aguila HL. Hematopoiesis is severely altered in mice with an induced osteoblast deficiency. *Blood*. 2004;103(9):3258-3264.

33. Winkler IG, Sims NA, Pettit AR, et al. Bone marrow macrophages maintain hematopoietic stem cell (HSC) niches and their depletion mobilizes HSCs. 2010;116(23):4815-4828.

34. Katayama Y, Battista M, Kao WM, et al. Signals from the sympathetic nervous system regulate hematopoietic stem cell egress from bone marrow. *Cell*. 2006;124(2):407-421.

35. Tanum G. The megakaryocyte DNA content and platelet formation after the sublethal whole body irradiation of rats. *Blood*. 1984;63(4):917-920. http://www.ncbi.nlm.nih.gov/entrez/query.fcgi?cmd=Retrieve&db=PubMed&dopt=Citation&list_uids=6367853

36. Marino R, Otsuru S, Hofmann TJ, et al. Delayed marrow infusion in mice enhances hematopoietic and osteopoietic engraftment by facilitating transient expansion of the osteoblastic niche. *Biol Blood Marrow Transplant*. 2013;19(11):1566-1573.

37. Méndez-Ferrer S, Michurina TV, Ferraro F, et al. Mesenchymal and haematopoietic stem cells form a unique bone marrow niche. *Nature*. 2010; 466(7308):829-834.

38. Winkler IG, Pettit AR, Raggatt LJ, et al. Hematopoietic stem cell mobilizing agents G-CSF, cyclophosphamide or AMD3100 have distinct mechanisms of action on bone marrow HSC niches and bone formation. *Leukemia*. 2012;26:1594-1601.

39. Hoggatt J, Mohammad KS, Singh P, et al. Differential stem- and progenitor-cell trafficking by prostaglandin E2. *Nature*. 2013;495(7441):365-369.

40. Chow A, Lucas D, Hidalgo A, et al. Bone marrow CD169+ macrophages promote the retention of hematopoietic stem and progenitor cells in the mesenchymal stem cell niche. *J Exp Med*. 2011;208(2):261-271.

41. Méndez-Ferrer S, Battista M, Frenette PS. Cooperation of β(2)- and β(3)-adrenergic receptors in hematopoietic progenitor cell mobilization. *Ann N Y Acad Sci*. 2010;1192:139-144.

42. Lee-Thedieck C, Rauch N, Fiammengo R, Klein G, Spatz JP. Impact of substrate elasticity on human hematopoietic stem and progenitor cell adhesion and motility. *J Cell Sci*. 2012;125(Pt 16):3765-3775.

43. Heller E, Fuchs E. Tissue patterning and cellular mechanics. *J Cell Biol*. 2015;211(2):219-231.

44. Spradling A, Drummond-Barbosa D, Kai T. Stem cells find their niche. *Nature*. 2001;414(6859):98-104.

45. Hamann J, Koning N, Pouwels W, et al. EMR1, the human homolog of F4/80, is an eosinophil-specific receptor. *Eur J Immunol*. 2007;37(10):2797-2802.

Downloaded from http://ashpublications.net/bloodadvances/article-pdf/1/27/2667/879379/advances008730.pdf by guest on 18 May 2024

46. Blaise D, Maraninchi D, Archimbaud E, et al. Allogeneic bone marrow transplantation for acute myeloid leukemia in first remission: a randomized trial of a busulfan-Cytoxan versus Cytoxan-total body irradiation as preparative regimen: a report from the Group d'Etudes de la Greffe de Moelle Osseuse. *Blood*. 1992;79(10):2578-2582.

47. Granados E, de La Cámara R, Madero L, et al. Hematopoietic cell transplantation in acute lymphoblastic leukemia: better long term event-free survival with conditioning regimens containing total body irradiation. *Haematologica*. 2000;85(10):1060-1067.

48. Socié G, Clift RA, Blaise D, et al. Busulfan plus cyclophosphamide compared with total-body irradiation plus cyclophosphamide before marrow transplantation for myeloid leukemia: long-term follow-up of 4 randomized studies. *Blood*. 2001;98(13):3569-3574.

49. Linsenmeier C, Thoennessen D, Negretti L, et al. Total body irradiation (TBI) in pediatric patients. A single-center experience after 30 years of low-dose rate irradiation. *Strahlenther Onkol*. 2010;186(11):614-620.

Downloaded from http://ashpublications.net/bloodadvances/article-pdf/1/27/2667/879379/advances008730.pdf by guest on 18 May 2024